EXPERIMENTAL STUDY ON THE INTERACTION BETWEEN BURGERS VORTEX AND SINGLE PARTICLE FOR MODELING OF A PARTICULATE TURBULENT FLOW

Yohsuke Tanaka
Department of Mechanical Engineering
Osaka University
Suita, Osaka, Japan
t_yohsuke@mupf.mech.eng.osaka-u.ac.jp

Takuya Tsuji
Department of Mechanical Engineering
Osaka University
Suita, Osaka, Japan
tak@mech.eng.osaka-u.ac.jp

Toshitsugu Tanaka
Department of Mechanical Engineering
Osaka University
Suita, Osaka, Japan
tanaka@mech.eng.osaka-u.ac.jp

ABSTRACT

In the present study, as an elementary physics for modeling a particulate turbulent flow, interactions between a single particle and a single Burgers vortex are observed by using 2D-PIV measurement. We used three kinds of particles which have particle Reynolds numbers ranged from 1258 to 2854. Their diameters are larger than the Kolmogorov scale. The vortex Reynolds number used is 79. Especially, we focus on the vorticity field and the superficial fluid divergence field induced by the particle motion on a cross-section perpendicular to the vortex axis. It is found that the maximum vorticity is increased when the particle pass through the forced vortex area, and the increase does not occur when the particle pass through the free vortex area.

INTRODUCTION

Turbulence modulation in particulate flows is one of the most interesting phenomena in multiphase flow. By adding small amount of particles to the flow, it have been found that the drastic change of characteristics of turbulent flow represented by turbulence intensities and Reynolds stress occurs (Tsuji, 1984, Rashidi, 1990, Squires, 1991, Fessler, 1994, Pan, 1996, Boivin, 1998, Ahmed, 2000). However, even if the research is limited in dilute particle-laden flows, the phenomenon is highly complicated, and is not yet understood essentially. Especially, the knowledge of the larger particle size than the smallest turbulence scale is insufficient due to difficulties in experimental measurements, theoretical analysis and numerical simulations.

On the other hand, it is found that coherent vortex structures play an important role in the momentum and energy transportation in turbulent flows (Vincent, 1991, Douady, 1991, Jimenéz, 1993, Frisch, 1995, Hosokawa, 1997). By using large scale direct numerical simulation, it is observed that the structures are composed of many vortex tubes, those having 5-10 times diameter of the smallest scale (Tanahashi, 2004). The diameter is independent of Reynolds number. The vortex tube is modeled by several theoretical vortices (Burgers, 1948, Lundgren, 1982, Hatakeyama, 1997, Kambe, 2000, Pullin, 2001, Kawahara, 2005). Burgers vortex among models has an exact solution of Navier-Stokes equation, and the vortex is the simplest model of the coherent structures.

To understand turbulence modulation, the elementary interaction between a particle and a vortex tube have been studied (Marcu, 1995, Raju, 1996, Kim, 1995, Kim, 1996, Niazmand, 2003, Sun, 2000). In conventional studies, the test cross-section perpendicular to the rotational axis has been observed (Marcu, 1995, Raju, 1996, Kim, 1995, Kim, 1996, Niazmand, 2003). In numerical simulations, the particle trajectory was mainly observed in case of the smaller particle than the vortex (Marcu, 1995, Raju, 1996). The drag and lift coefficient were observed in case of the larger particle than the vortex (Kim, 1995, Kim, 1996, Niazmand, 2003). However, there are no discussions on the influence of the particle motion on the vortex in these observations. On the other hand, in experimental measurements, there is only the observation of the interaction between the vortex tube and the vortex shedding from particle fixed at the support (Sun, 2000).

The phenomena of turbulence modulation in particulate flows are essentially three dimensional motion, and the particle does not only move on the cross section. Moreover, it is preferable that the support is removed to consider the influence of the particle on the vortex. In the preset study, we generated Burgers vortex which had the axis in the gravitational direction, and observed the influence of the particle, gravitational settling near the rotational axis, on the vortex in particle passing through the forced and the free vortex area. We focused on the stable vortex having about several times diameter of the particle.

BURGERS VORTEX

Definition of Burgers vortex

Burgers vortex consists of a vortex tube superposed on an axisymmetric stagnation point flow. The fluid is incompressible. In the cylindrical coordinate (r, θ, z), the solution is written as (Burgers, 1948)

$$u(r, \theta, z) = (-\alpha r, v_\theta(r), 2\alpha z), \tag{1}$$

where, α is the strain rate of the background flow field. The circumferential velocity v_θ is given by

$$v_\theta(r) = \frac{\Gamma}{2\pi r}\left\{1 - exp\left(-\frac{r^2}{l_b^2}\right)\right\}. \tag{2}$$

Γ is the circulation. ν is the viscosity of the fluid, and l_b (=

$\sqrt{2\nu/\alpha}$) is the Burgers length scale. The maximum value of $v_\theta(r)$ is found at the position $r \approx 1.12 l_b$ from Eq. (2) (Rott, 1958). Substituting Eqs.(1) and (2) into the vorticity equation, the solution of the vorticity ω is given as follows

$$\omega = (0, 0, \frac{\Gamma}{\pi l_b^2} exp\left(- \frac{r^2}{l_b^2} \right)). \quad (3)$$

Relation between Burgers vortex length scale and Kolmogorov scale

Assuming that the rate of straining α is of the order of $2\alpha \approx v_{rms}/\lambda$, the relation between Burgers vortex length scale l_b and Kolomgorov scale η is given as follows (Kambe, 2000)

$$\begin{aligned} l_b &= (2\nu/\alpha)^{1/2} = (4\nu\lambda/v_{rms})^{1/2} \\ &= (240\nu^3/\epsilon)^{1/4} \approx 3.9\eta, \end{aligned} \quad (4)$$

where λ is Taylor microscale, v_{rms}, rms velocity and ϵ, the rate of dissipation of energy, respectively. The radius of Burgers vortex is defined as $r \approx 1.12 l_b$ (Rott, 1958, Tanahashi, 2004). Substituting this radius into Eq. (4), the diameter d_v of Burgers vortex is given by 8.81η.

EVALUATION OF THE INFLUENCE OF PARTICLE ON THE FLOW

In this study, we measured a flow field on a cross-section perpendicular to the vortex axis. To make a quantitative evaluation of the influence of the particle on the flow field on the measuring plane, fields of superficial divergence and vorticity on the plane are obtained. The vortex field and in cylindrical coordinate (r, θ, z) used are illustrated in Fig. 1. The superficial divergence on $r\theta$ plane induced by the particle motion is expressed as $\mathrm{div}_{r\theta}u$, and defined by

$$\mathrm{div}_{r\theta}u = \frac{1}{r}\frac{\partial(ru_r)}{\partial r} + \frac{1}{r}\frac{\partial u_\theta}{\partial \theta}. \quad (5)$$

As the flow can be assumed incompressible, $\mathrm{div}_{r\theta}u$ is given as follows using the continues equation

$$\mathrm{div}_{r\theta}u = -\frac{\partial u_z}{\partial z}. \quad (6)$$

The relation of Eq. (6) is illustrated in Fig. 1. Superficial outlet flow ($\mathrm{div}V(r,\theta) > 0$) is induced by the particle approaching the plane ($\partial u_z/\partial z < 0$), and superficial inlet flow ($\mathrm{div}V(r,\theta) < 0$) is induced by the particle leaving $r\theta$ plane ($\partial u_z/\partial z > 0$).

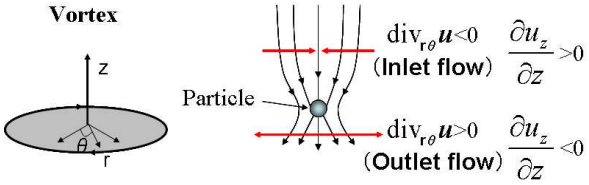

Figure 1: A vortex and a single particle

BURGERS VORTEX GENERATOR AND CONDITIONS

Burgers vortex generator

Figure 2 shows the principle of Burgers vortex generator. The lower part of the axisymmetric stagnation-point flow is generated by four circulation pumps in the water tank (0.15 m !_0.15 m !_1 m). The water circulates from topside of the water tank to the orifice. The vortex motion is generated by the rotating disk (60 mm in diameter! $1000 rpm).

The schematic diagram of the experimental setup is shown in Fig. 3. Burgers vortex is measured from the observation window installed at the lower part of the water tank using PIV measurement. The conditions of PIV are presented in Table 1. The test cross-section of the vortex which is illuminated by the laser light sheet, is located at the distance of 0.15 m from the orifice. The CMOS camera starts to capture images when the particle is detected by the area sensor (as shown in the magnified view of Fig. 3).

The vertical component of the particle velocity is measured by the particle velocimetry (4 in Fig. 3) set 50 mm above the test cross-section. The particle velocimetry is composed of a couple of area sensors (sampling rate: 12.5 kHz) and a digital signal recorder which records the output of the area sensors. The particle velocity is calculated by the spacing between the area sensors (20 mm) and the time delay of the signals.

Particle dispenser is installed 0.47 m above the test cross-section, and the particle passes through the test cross-section with the terminal velocity for the present conditions. The dispenser is mounted on the X stage (±15 mm) to adjust the particle initial position. The particle dispenser is composed of an aluminum pipe (5 mm in outside diameter, 4 mm in internal diameter), and a couple shutters connected the shape memory alloy wire (0.25 mm in diameter, Biometal fiber: Toki corporation) as shown in Fig. 4. When applying current, the shutters are opened by contraction of the wire and the particle is released. The standard deviation of particle passing through positions is 8.87 mm by using this dispenser.

Table 1: Observation conditions

Vector componet	2 dimensional, 2 componet
Observation area	W61×H61 mm
Interrogation area	W0.9×H0.9 mm
Lens	f=105 mm, f#=2.8, distance 1.3 m
Camera	CMOS, 512×512pixel×8bit,250Hz
Tracer	SP20SS with Rhodamin B, ϕ50μm
Lighting	Ar laser, CW, 2.8W, sheet 2 mm
Analysis	Iterative PIV using gradient method
False vector	neural network
Vector number	57×57vectors×600frames,(120min)
PC	CPU/2.79GHz, RAM/1GB HDD/250GB

Burgers vortex condition

Vortex Reynolds number defined by $Re_\Gamma = \Gamma_0/\nu$ is 79 from the measured velocity field, where the circulation Γ_0 is obtained in the area $r/l_b < 1.12$. The flow velocity at the orifice installed to stretch the vortex (Fig. 2 and Fig. 3) is 7.1 mm/sec.

We estimated Kolmogorov scale $\eta = (\nu^3/\epsilon)^{1/4}$, velocity $v_K = (\epsilon\nu)^{1/4}$ and time $\tau_K = (\nu/\epsilon)^{1/2}$ (Davidson, 2004). The maximum circumferential velocity is found at $r \approx 1.12 l_b$ (Rott, 1958). Therefore, the Burgers length scale l_b is estimated to be 8.96 mm from the distribution of the fluid velocity (Fig. 6). Substituting this value into Eq. (4), we obtain $\eta = 2.28$ mm. Kolmogorov velocity and time based on this η and viscosity ν are $v_K = 0.36$ mm/sec, $\tau_K = 4.2$ sec, respectively.

Particle condition

Equation (6) shows that $\mathrm{div}_{r\theta}u$ is controlled by $\frac{\partial u_z}{\partial z}$. To observe the influence of the particle on Burgers vortex, we used three kinds of particle (A,B,C) as presented in Table 2. The diameter of each particle is almost same, however the density ρ_p is different.

To estimate particle motions on the vortex tracking, Stokes number is defined as follows

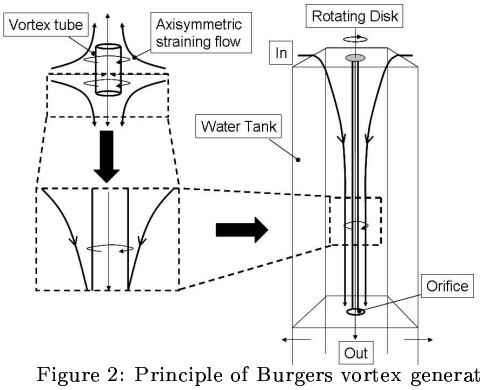

Figure 2: Principle of Burgers vortex generator

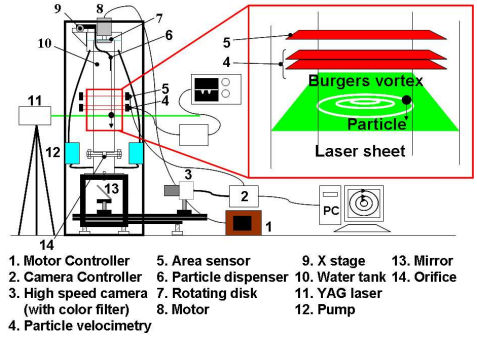

Figure 3: Burgers vortex generator

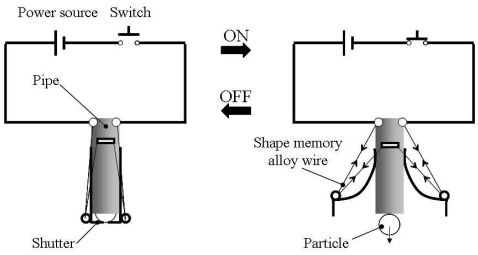

Figure 4: Particle dispenser

$$St = \frac{\tau_p}{\tau_f}. \quad (7)$$

Here, τ_p and τ_f are the particle response time and the particle's residence time in the vortex. In the present study, the particle is falling inside the vortex tube. Therefore, τ_f is defined as the time interval between the moment of releasing particle and the moment of particle reaching the test cross-section. The particle response time is given by

$$\tau_p = \frac{2d_p^2(2\rho_p + \rho_f)}{3\mu Re_{p\theta} C_d}. \quad (8)$$

In Eq. (8), virtual mass force is considered, because the particle density ρ_p is only about 9 times in comparison with the fluid density ρ_f (Tanaka, 2003). The range of Particle Reynolds number ($Re_{p\theta} = d_p V_{\theta max}/\nu$! $V_{\theta max}$:maximum circumferential velocity) shown in Table 2 is much larger than the Stokes drag range. Therefore, Stokes drag is modified by the drag coefficient (C_d ! $10^{-2} < Re_{p\theta} < 3 \times 10^5$) (Khan, 1987)

$$C_d = (2.25 Re_{p\theta}^{-0.31} + 0.36 Re_{p\theta}^{0.06})^{3.45}. \quad (9)$$

Stokes number indicates the degree of the tracking the vortex for the particle motion. For $St \ll 1$, the particle will track the vortex motion, and the particle falling gravitationally is in spiral motion falls. For $St \gg 1$, the particle will move essentially independent of the vortex motion. According to the obtained value of Stokes number, all particle conditions become in the condition of particle tracking the vortex. Moreover, the velocity of each particle reaches almost terminal velocity by comparing the averaged particle velocity $\overline{V}_{pz}$ (sample number=50) with V_{pzt} calculated by applying Eq. (9). Here, the particle Reynolds number is defined as $Re_{pz} = \overline{V}_{pz} d_p/\nu$, the averaged particle velocity is chosen as the representative velocity. From these results, it is found that each particle tracks the vortex motion.

Table 2: Particle conditions

Particle	A	B	C
Material	Glass	Alumina	Steal
$Re_{p\theta}$ (-)	5411	5517	5583
St (-)	1.23×10^{-2}	2.14×10^{-2}	7.49×10^{-2}
τ_p (sec)	5.97×10^{-2}	6.02×10^{-2}	8.86×10^{-2}
τ_f (sec)	1.34	1.03	0.64
d_p/η (-)	1.27	1.29	1.31
d_p (mm)	2.9±0.17	2.95±0.10	3.00±0.00
$V_\theta max$ (m/sec)	1.49		
ρ_p (kg/m^3)	2594	3557	8128
Re_{pz} (-)	1258	1815	2854
$\overline{V}_{pz}$ (m/sec)	0.36	0.49	0.82
V_{pzt} (m/sec)	0.36	0.48	0.83

Validity of the generated Burgers vortex

Figure 5 indicates the time-averaged vorticity distribution (0.4sec, 100frames). The circularity value of the vortex is 0.90 at the contour line with respect to the maximum value of the circumferential velocity ($r/l_b \approx 1.12$). Here, a circularity value of 1.0 indicates a perfect circle. The circularity is measured by the image processing software (Image J).

The measured distributions of the circumferential velocity and the vorticity are compared with the distributions of the exact solutions Eqs. (2) and (3) as shown in Fig. 6. ω^* and V_θ^* are non-dimensionalized by the maximum values of the circumferential velocity and the vorticity, respectively. Experimental results agree with the theoretical results. Therefore, it is confirmed that the present setup generates Burgers vortex. It is observed that the vortex area is divided into the forced vortex and the free vortex area at $r/l_b \approx 1.12$ from the velocity distribution in Fig. 6 (Rankine, 1921).

Additionally, we evaluate the time stability of the rotational axis position. The position is defined as the point of the maximum vorticity. The position is measured by the longer time interval (0.4sec) than the interval of particle passing through (0.048sec). The standard deviation of the position is obtained 0.84mm. This value are smaller than the diameter of the vortex 20.0mm. Hence, it is found that the position is stable.

QUANTITATIVE ESTIMATION AND VISUALIZATION OF THE INFLUENCE OF PARTICLE ON THE VORTEX

The influence of the particle is expressed by the vorticity of Burgers vortex and the superficial divergence of particle motion in Fig. 1. (a) in Figure. 7 shows the velocity field when particle B set $z/l_b = 0.44$ above the test cross-section. (b) shows the positioning relation between the particle and the cross section. The circle in (a) is correspond to the particle size and the pass through-position projected to the cross section. $z/l_b = 0$ in (b) indicates the test cross-section. The distance z/l_b between the particle and the cross-section is derived from the product of the measured particle velocity and the number of frames from the particle passing through

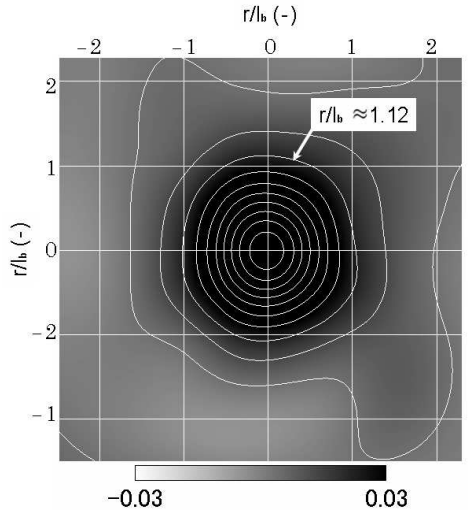

Figure 5: Vorticity field of Burgers vortex

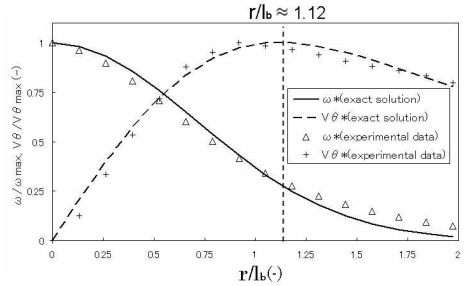

Figure 6: Distributions of fluid circumferential velocity and vorticity

frame to an observation frame. (c) and (d) show the vorticity field $\omega_z(r,\theta)$ and the superficial divergence field $\mathrm{div}_{r\theta}u$.

The correspondence of a position between the vorticity and the divergence is incomprehensible as shown in (c) and (d) of Fig. 7. Then, to combine these figures into one, BVD (Balance between the Vorticity and Divergence) is defined as

$$\mathrm{BVD}(r,\theta) \quad = \quad |\omega_z(r,\theta)| - |(\mathrm{div}_{r\theta}u)(r,\theta)|. \qquad (10)$$

(a) in Figure 8 shows $\mathrm{BVD}(r,\theta)$ field. By comparing (c) and (d) of Fig. 7 with Fig. 8, it is observed that the white area of the high divergence and the black area of the high vorticity are simultaneously displayed in (a) of Fig. 8. (b) in Figure. 8 shows the value on the dashed line in (a) which crosses the maximum value (BVD_{max}) and the minimum value (BVD_{min}). In next chapter, we focus on the vorticity of Burgers vortex and the superficial divergence of the particle motion and observe the BVD distribution.

EXPERIMENTAL RESULTS

Change of BVD distribution and the distance between the particle and test cross-section

In cases of the particle A passing through the forced vortex area and the passing through the free vortex area, Figure 9 presents the change with respect to z/l_b of BVD fields and the velocity field. To observe the change of the influence of the particle position in z direction on the vortex, we focus on the maximum values of the vorticity $\omega_{z\ max}$ and the superficial divergence $\mathrm{div}_{r\theta}u_{max}$. Figure 10 shows the change of $\omega_{z\ max}/\overline{\omega_{z\ max}}$ and $\mathrm{div}_{r\theta}u_{max}/\overline{|\mathrm{div}_{r\theta}u_{max}|}$ corresponding to the results of Fig. 9. Each value is non-dimensionalized by the time averaged value without the influence of the particle motion.

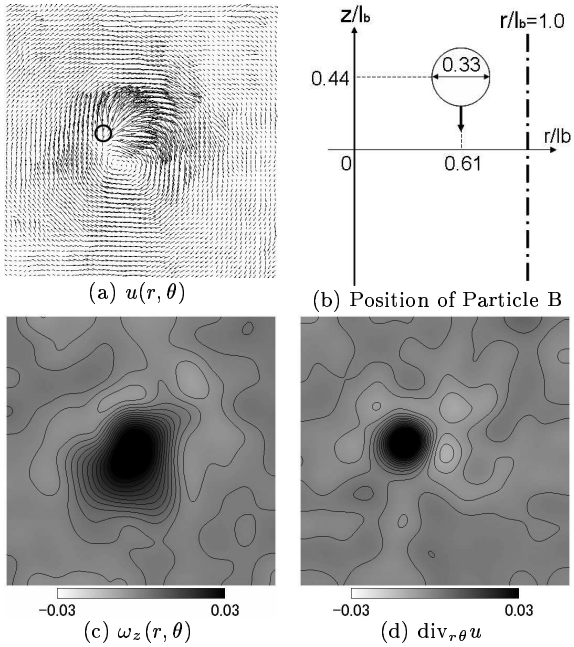

(a) $u(r,\theta)$ (b) Position of Particle B

(c) $\omega_z(r,\theta)$ (d) $\mathrm{div}_{r\theta}u$

Figure 7: Distributions of the vorticity and the superficial divergence

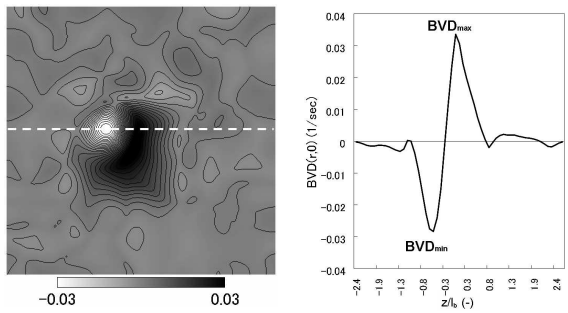

(a) $\mathrm{BVD}(r,\theta)$ (b) BVD on dash line

Figure 8: BVD field

Z-direction velocity u_z is close to the particle velocity as the particle approaches to the cross-section. From the relation of Eq. (6), the outlet flow is observed at $z/l_b = 0.58$ in (a) and (b) of Fig. 9, and the peak value of the superficial divergence is observed in (a) and (b) of Fig. 10. The velocity u_z is nearly equal to the particle velocity at $z/l_b = 0$ of the particle passing through, and $\partial u_z/\partial z = 0$ is derived from Eq. (6), and the peak value is not observed in Fig. 10. As particle leaves the cross-section, the inlet flow is induced at $z/l_b = -0.58$, and the peak is observed again.

In case of the particle passing through the forced vortex area indicated in (a) of Fig. 10, the increase of the maximum vorticity is observed at $z/l_b = 0.58$ and $z/l_b = -0.58$ corresponding to the peaks of the superficial divergence as observed in (a) of Fig. 9 The reason of the increase is not understood well enough, however it is found that the superficial divergence is synchronized with the increase of the maximum vorticity.

On the other hand, in case of the particle passing through the free vortex area, the increase of the maximum vorticity is not observed at $z/l_b = 0.58$ and $z/l_b = -0.58$ corresponding to the peaks of the superficial divergence as observed in (b) of Fig. 9. The same tendency is observed in cases of particle B and particle C.

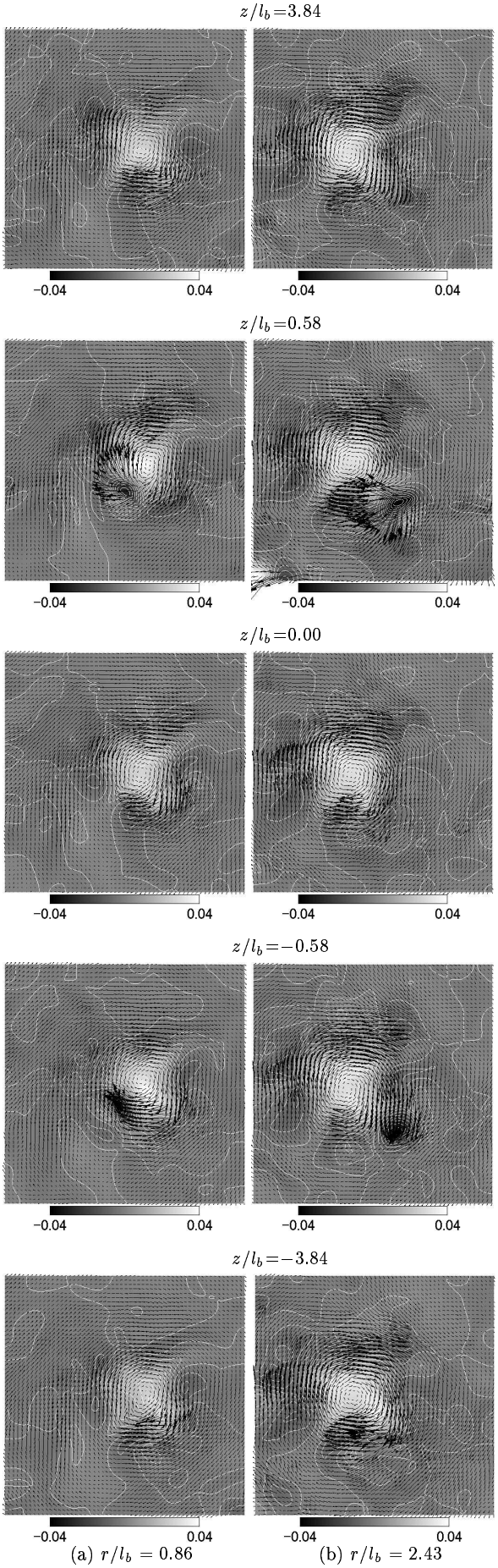

(a) r/l_b = 0.86 (b) r/l_b = 2.43

Figure 9: $u(r,\theta)$ and BVD(r,θ) for each z/l_b (Particle A)

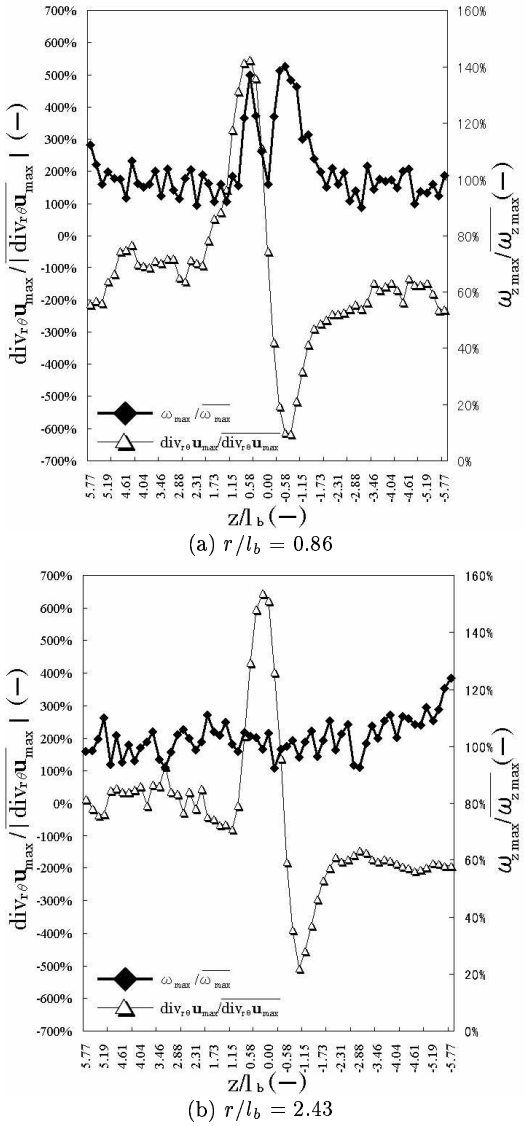

(a) r/l_b = 0.86

(b) r/l_b = 2.43

Figure 10: $\omega_{z\ max}$ and $\mathrm{div}_{r\theta}u_{max}$ for each z/l_b (Particle A)

The influence of the position of the particle passing through on the vortex

The increase of the maximum vorticity $\omega_{z\ max}$ is induced by the superficial divergence at the position of the particle passing through. Figure 11 shows the increase with respect to the different particle velocity on three kinds of particles (A,B,C). Here, the increase rate of the maximum vorticity is defined as $((\omega_{z\ max} - \overline{\omega_{z\ max}})/\overline{\omega_{z\ max}})$. $\overline{\omega_{z\ max}}$ is the time averaged value without the particle.

As observed in (a) of Fig. 10, $\omega_{z\ max}$ is increased by synchronized with the superficial divergence in case of the particle passing through the forced vortex area ($r/l_b < 1.12$). In contrast, $\omega_{z\ max}$ is not increased in case of the particle passing through the free vortex area ($r/l_b > 1.12$).

There is a possibility that $\omega_{z\ max}$ is more increased by the higher particle velocity if the superficial divergence causes the increase of $\omega_{z\ max}$. However, the increase of $\omega_{z\ max}$ is small by the present conditions with different particle terminal velocities.

CONCLUSIONS

In the present study, Burgers vortex is generated in the vertical water tank. The rotational axis is directed in the

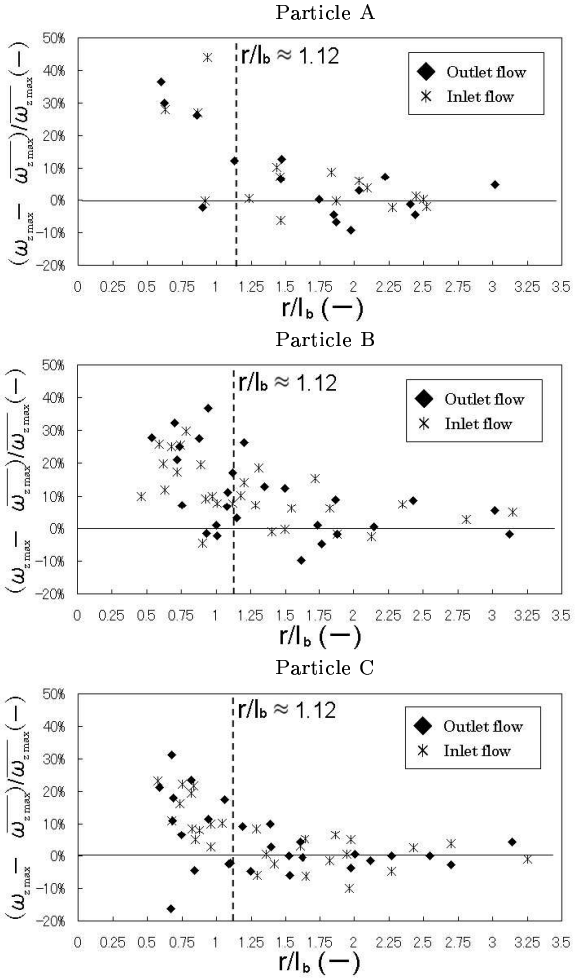

Figure 11: Influence of particle's passing position on the change of $\omega_{z\ max}$

gravitational direction. The influence of the gravitational settling near the rotational axis of the particle on the vortex is experimentally measured. The flow field of the test cross-section perpendicular to the axis is measured by PIV measurement.

The time until particle reaching the cross section is longer than the particle response time, and the particle motion is in an equilibrium state with respect to the vortex motion. The particle Reynolds number based on the particle terminal velocity is in the range of 1258 to 2854. The main results are as follows:

(1) It is confirmed that the developed setup generates Burgers vortex by comparing the measured distributions of the vorticity and the circumferential velocity with Burgers vortex's ones.

(2) The change of the distributions of the vorticity and the superficial divergence induced by the particle passing through are observed in the test cross-section perpendicular to the rotational axis. In case of the particle passing through the forced vortex area, the maximum vorticity is increased.

(3) The change of the maximum vorticity by the particle passing through the forced vortex area is synchronized with the superficial divergence in the test cross-section perpendicular to the rotational axis, and the increase rate of the maximum vorticity becomes the maximum value with respect to the peak of the superficial divergence.

(4) The increase of the maximum vorticity described in (2) is not observed in case of the particle passing through the free vortex area.

ACKNOWLEDGMENT

One of the authors (Y. Tanaka) has been supported by the Research Fellowships of the Japan Society for the Promotion of Science for Young Scientists.

REFERENCES

Ahmed,A.M. et al., 2000, *Phys.Fluids*, Vol. 12-11, pp. 2906-2930.

Boivin,M. et al., 1998, *J.Fluid Mech.*, Vol. 375, pp. 235-263.

Burgers,J.M., 1948, *Adv.Appl.Mech.*, Vol. 1, pp. 171-199.

Davidson,P.A, 2004, *turbulence*, OXFORD University Press, pp. 76-80.

Douady,S. et al., 1991, *J.Fluid Mech.*, Vol. 67-8, pp. 983-987.

Fessler,J.R. et al., 1994, *Phys.Fluids*, Vol. 6-11, pp. 3742-3749.

Frisch,U., 1995, *Turbulence*, Cambridge University Press, pp. 182-188.

Hatakeyama,N. et al., 1997, *Phys. Rev. Lett*, Vol. 79-7, pp. 1257-1260.

Hosokawa,I. et al., 1997, *J.Phys.Soc.Jpn.*, Vol. 66-10, pp. 2961-2964.

Jiménez,J. et al., 1993, *J.Fluid Mech.*, Vol. 255, pp. 65-90.

Kambe,T. et al., 2000, *Fluid Dyn. Res.*, Vol. 27, pp. 247-267.

Khan.A.R. et al., 1987, *Chem. Eng. Comm*, Vol. 62, pp. 135-150.

Kawahara,G., 2005, *Phys. Fluids*, 17, 055111-1-055111-13.

Kim,I. et al., 1995, *J.Fluid Mech*, Vol. 288, pp. 123-155.

Kim,I. et al., 1996, *Int. J. Multiphase Flow*, Vol. 23-1, pp. 1-23.

Lundgren,T.S., 1992, *Phys. Fluids*, Vol. 25-12, pp. 2193-2203.

Marcu,B. et al., 1995, *Phys.Fluids*, Vol. 7-2, pp. 400-410.

Niazmand,H. and Renksizbulut,M., 2003, *Part. Part. Syst. Charact.*, Vol. 20, pp. 47-61.

Pan,Y. and Banerjee,S., 1996, *Phys.Fluids*, Vol. 8-10, pp. 2733-2755.

Pullin,D.I. et al., 2001, *Phys. Fluids*, Vol. 13-9, pp. 2553-2563.

Raju,N. and Meiburg,E., 1996, *Phys.Fluids*, Vol. 9-2, pp. 299-314.

Rankine.W.J.M, 1921, *A Manual Applied Mechanics 21ed*, C. Griffin, pp. 574-578.

Rashidi,M. et al., 1990, *Int. J. Multiphase Flow*, Vol. 16-6, pp. 935-949.

Rott,N., 1958, *Z. angew. Math. Phys.*, Vol. 9-5-6, pp. 543-553.

Squires,K.D. and Eaton,J.K., 1991, *Phys.Fluids A*, Vol. 3-3, pp. 1169-1178.

Sun,M. et al., 2000, *Trans.ASME*, Vol. 122, pp. 560-568.

Tanahashi,M. et al., 2004, *Int. J. Heat and Fluid Flow*, Vol. 25, pp. 331-340.

Tanaka,Y. et al., 2003, *Int. J. Multiphase Flow*, Vol. 29, pp. 361-373.

Tsuji,Y. et al., 1984, *Int. J. Multiphase Flow*, Vol. 139, pp. 417-434.

Vincent,A. et al., 1991, *J.Fluid Mech.*, Vol. 225, pp. 1-20.